

---

# Transfer Automatic Machine Learning

---

Catherine Wong<sup>1</sup> Neil Houlsby<sup>2</sup> Yifeng Lu<sup>2</sup> Andrea Gesmundo<sup>2</sup>

## Abstract

Building effective neural networks requires many design choices. These include the network topology, optimization procedure, regularization, stability methods, and choice of pre-trained parameters. This design is time consuming and requires expert input. Automatic Machine Learning aims to automate this process using hyperparameter optimization. However, automatic model building frameworks optimize performance on each task independently, whereas human experts leverage prior knowledge when designing a new network. We propose Transfer Automatic Machine Learning, a method to accelerate network design using knowledge of prior tasks. For this, we build upon reinforcement learning architecture design methods to support parallel training on multiple tasks and transfer the search strategy to new tasks. Tested on NLP and Image classification tasks, Transfer Automatic Machine Learning reduces convergence time over single-task methods by almost an order of magnitude on 13 out of 14 tasks. It achieves better test set accuracy on 10 out of 13 tasks NLP tasks and improves performance on CIFAR-10 image recognition from 95.3% to 97.1%.

## 1. Introduction

Designing neural networks that perform well on a task often requires an extensive process of iterative engineering and tuning of the architecture and training algorithm. These design decisions are usually made by human experts, guided by a combination of intuition, grid search, and heuristics.

Automatic Machine Learning (AML) algorithms aim to find the best performing learning algorithm with minimal human intervention. Many AML methods have been proposed, including random search (Bergstra & Bengio, 2012), performance modelling (Bergstra et al., 2011; 2013), Bayesian optimization (Snoek et al., 2012), genetic algorithms (Real et al., 2017; Miikkulainen et al., 2017) and reinforcement learning (Baker et al., 2017; Zoph & Le, 2017).

Recent advances in AML have made promising strides to-

wards accelerating or even eliminating the manual parameter search. For example, architecture search using deep reinforcement learning (RL) has successfully discovered novel network architectures that rival the best human-designed architectures on challenging image classification tasks (Zhong et al., 2018; Zoph et al., 2017).

However, applying AML to each new task independently requires building and training many networks to learn how to construct the best models from scratch. For complex models this requires vast computations resources; Zoph & Le (2017) report the use of 800 concurrent GPUs. Human experts, on the other hand, can design and tune networks based on knowledge about underlying dependencies in the search space and experience with prior tasks. We therefore aim to automatically learn and leverage the same information.

Many AML methods use generic optimization algorithms, such as random search, genetic algorithms, or Bayesian optimization. It is hard to transfer prior knowledge onto new problems with a generic optimization procedure. We exploit the fact that deep reinforcement learning based AML algorithms learn an explicit parameterization of the search, via the RL policy. Using this, we present Transfer AML, a method to accelerate automatic design of networks on new tasks based on knowledge gained from previous tasks. Transfer AML is based upon policy gradient methods shown to generate performant architectures (Zoph & Le, 2017; Bello et al., 2017), optimization procedures (Bello et al., 2017) and activation functions (Prajit Ramachandran, 2018).

We first present an approach to perform neural AML on multiple tasks simultaneously. Multitask AML learns both hyperparameter choices common to multiple tasks, as well as specific configurations for individual problems. Multitask AML also learns representations for each task, which may be used to quantify their similarity. We then show that after transferring from this prior experience on multiple tasks we improve convergence on new tasks, reducing the computation time required to converge during optimization by an order of magnitude on 13 out of 14 tasks. Transfer AML produces better models than single task learning on 10 out of 13 NLP tasks. It also outperforms a competitive single task AML model on CIFAR-10, increasing test-set accuracy from 95.3% to 97.1% and converging substantially faster.

## 2. Methods

We build our Transfer AML method on top of Neural Architecture Search (Zoph & Le, 2017). In this section we first review Neural Architecture Search. We then present our architecture for performing simultaneous multitask training, and its subsequent use for transfer learning.

### 2.1. Neural Architecture Search

Neural Architecture Search uses deep reinforcement learning to generate model designs that maximize expected performance on a given task. The framework consists of two components: the controller model and the child models. At every iteration of training, the controller generates network configurations. These configurations define the architecture of the child models. The child models are trained and evaluated on the machine learning task at hand. The performance on the validation set of the child network is used as a reward to update the controller through a policy gradient algorithm.

The controller is an RNN that generates a sequence of discrete actions. Each action specifies a design choice; for example, if the child models are CNNs, these choices could include the filter heights, widths, and strides. An RNN allows dependencies between the design choices to be learned. The model is autoregressive, like a language model: the action taken at each time step is fed into the RNN as input for the next time step. The recurrent state of the RNN maintains a history of the design choices taken so far. The original Neural Architecture Search performed a search over a space of strictly architectural parameters. Other hyperparameters, such as those for the controller of the learning algorithm, were chosen by hand. In this work we use the controller to choose the architecture, optimization hyperparameters and make other design decisions such as which pre-trained embedding layers to use.

### 2.2. Multitask Training

We next describe our approach to Multitask Automatic Machine Learning, which allows simultaneous model search over multiple tasks. We first define a generic search space that is shared across all tasks. Many deep learning models require the same common design decisions, such as choice of network depth, learning rate, and number of training iterations. By defining a generic search space that contains many architecture and hyperparameter choices, the controller can generate a wide range of models applicable to many common machine learning tasks. Multitask training over this space can then allow the controller to learn broadly applicable relationships between search space actions by leveraging shared behaviour across tasks.

We propose a controller capable of simultaneous multitask training through two key features.

**Learned task representations** The multitask AML controller is trained simultaneously on a set of tasks. To generate different network configurations for each task, we map each task to a unique embedding. We then condition the generation of network configurations on the task by feeding the task embedding into the RNN controller at every time step. In single task training of Neural Architecture Search, the action at each time step is fed into the next time step via an embedding layer. In multitask training, the task embedding is concatenated to the embedding of the previous action and is fed into the input of the RNN. We also add a skip connection between the concatenated action/task embedding and the output of the RNN. This ease the learning of the unconditional component of the action distributions.

During training, for each trial the controller samples a task uniformly. The task embeddings are the only task-specific parameters, they are initialized randomly and trained jointly with the controller. Figure 1 depicts the architecture of the controller.

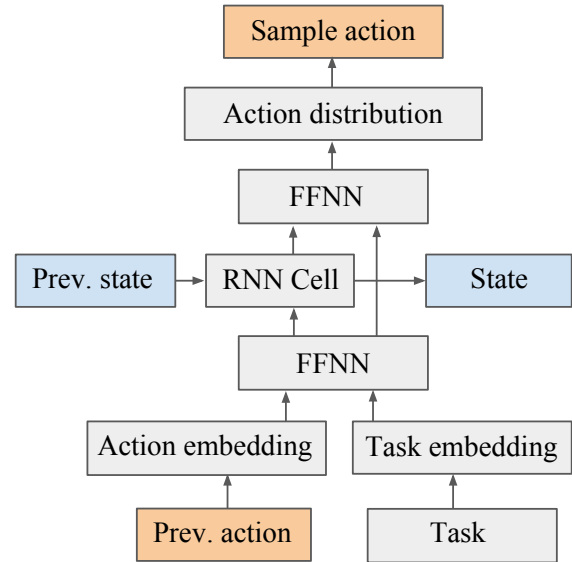


Figure 1. A single time step (action) of the recurrent multitask AML controller. The task embedding is concatenated with the embedding of the action sampled at the previous timestep and passed into the controller RNN. All parameters, other than the task embeddings, are shared across tasks.

**Task-specific baseline and normalization** We train the controller using policy gradient methods. Each task can define a different performance metric to be used as reward. The reward affects the amplitude of the gradients applied to update the controller’s policy,  $\pi$ . To learn effectively on differing tasks, we need to ensure that the distributions

of each task rewards are scaled to have same mean and variance.

The mean of each task’s reward distribution is centered on zero by subtracting the expected reward for the given task. The centered reward, or advantage,  $A_\tau(m)$ , of a model,  $m$ , applied to a task,  $\tau$ , is defined as the difference between the reward obtained by the model,  $R_\tau(m)$ , and the expected reward for the given task,  $b_\tau = \mathbb{E}_{m \sim \pi}[R_\tau(m)]$ :

$$A_\tau(m) = R_\tau(m) - b_\tau$$

$b_\tau$  is commonly referred to as the baseline. Subtracting a baseline is a standard technique in policy gradient algorithms used to reduce the variance of the parameter updates (Greensmith et al., 2004).

The variance of each tasks reward distribution is normalized by dividing the advantage by the standard deviation of the reward:

$$A'_\tau(m) = \frac{R_\tau(m) - b_\tau}{\sigma_\tau}$$

Where  $\sigma_\tau = \sqrt{\mathbb{E}_{m \sim \pi}[(R_\tau(m) - b_\tau)^2]}$ . We refer to  $A'$  as the normalized advantage.

In policy gradient, the gradient update to the parameters to the policy  $\theta$  is the product of the advantage and expected derivative of the log probability of sampling an action:

$$A'_\tau(m) \mathbb{E}_\pi[\nabla_\theta \log \pi_\theta(m)]$$

The normalizing the advantage can therefore be seen learning using an adaptive learning rate for each task.

We estimate a different baseline and standard deviation for each task. In practice, we compute  $b_\tau$  and  $\sigma_\tau$  using exponential moving averages over the sequence of rewards. Using the normalized advantage to scale the gradients allows to use a distinct performance metric as a reward for each task without compromising the balance of the gradients updates for each task.

### 2.3. Transfer Learning

Given the multitask AML controller, performing transfer learning is straightforward. The pre-trained controller learns a prior over generic architectural and parameter choices, along with task-specific decisions encoded in the task embeddings. Given a new task, one can significantly speed up exploration by leveraging the learned biases about what combinations of parameter choices worked well together. By learning an embedding for the new tasks, the controller can then learn a representation that biases towards actions that performed well on similar tasks.

To perform transfer we simply to initialize the generic parameters of the controller for the new task with the pre-trained multitask AML controller. We add a new randomly initialized task embedding for the new task. The controller weights and the new task embedding are then updated jointly with standard policy gradient steps.

### 3. Related Work

The complexity of model engineering in machine learning is widely recognized. Previous works propose a variety of optimization methods to search over the large space of model parameters, architectures, and hyperparameters, including random search over the architecture space (Bergstra & Bengio, 2012), parameter modeling (Bergstra et al., 2013), meta-learned model hyperparameter initialization (Feurer et al., 2015), deep-learning based tree searches over a pre-defined model-specification language (Negrinho & Gordon, 2017), and direct learning of gradient descent optimizers (Wichrowska et al., 2017). More recently, an emerging body of modern neuro-evolution research has adapted genetic algorithms as an alternate optimization method for these complex searches (Conti et al., 2017), including to set the parameters of existing deep networks (Such et al., 2017), evolve image classifiers (Real et al., 2017), and evolve deep neural networks in general (Miikkulainen et al., 2017).

Our work, however, is most closely related to the Neural Architecture Search (NAS) method introduced in (Zoph & Le, 2017). NAS was applied to construct Convolutional Neural Networks (CNNs) for the CIFAR-10 task and Recurrent Neural Networks (RNNs) for the Penn Treebank tasks. Later work by the same authors attempted to address the computational cost of using Neural Architecture Search for more challenging tasks (Zoph et al., 2017). To engineer a convolutional architecture for ImageNet classification, this paper demonstrated that it was possible to train the NAS controller on the simpler, proxy CIFAR-10 task and then transfer the architecture to ImageNet classification by stacking it. However, this work did not attempt to transfer the controller model itself across multiple tasks, relying instead on the human expert intuition that additional network depth was necessary for the more challenging classification task. Additionally, the final generated architectures required additional tuning to choose hyperparameters, such as the learning rate, before evaluation on the test set. Other recent publications have also applied RL to automate architecture generation. These include MetaQNN, a Q-learning algorithm that sequentially chooses CNN layers (Baker et al., 2016). MetaQNN uses an aggressive exploration to reduce search time, though it can cause the resulting architectures to underperform. Cai et al. (2017) also propose an RL agent that transforms existing architectures incrementally to avoid generating entire networks from scratch.

Our work draws on prior research in transfer learning and simultaneous multitask training. Transfer learning has been shown to achieve excellent results as an initialization method for deep networks, including for models trained using RL (Yosinski et al., 2014; Sharif Razavian et al., 2014; Zhan & Taylor, 2015). Recent meta-learning research has broadened this concept to learn generalizable representations across classes of tasks (Finn et al., 2017; Mishra et al., 2017). Simultaneous multitask training can also facilitate learning between tasks with a common structure, though effectively retaining knowledge across tasks is still an active area of research (Kirkpatrick et al., 2017; Teh et al., 2017).

## 4. Experiments

Our main result demonstrates that with transfer learning we accelerate convergence of AML on a variety of NLP and image datasets. Transfer AML achieves a equivalent reward equal to single-task AML in an order of magnitude fewer trials on many datasets (Table 2), and generates models with higher accuracy given a fixed budget on text (Table 3) and image (Figure 3) data. We also show that by training simultaneously on multiple tasks, the amortized sample efficiency is improved.

### 4.1. Setup

**Child models** We aim to fully automate neural network design, tuning and training. We therefore define a search space that includes most configuration parameters for a neural architecture and training algorithm. Note, constructing the space needs human input, but we choose very wide parameter ranges so minimal domain expertise is injected. Our class of child models is two-tower feedforward neural networks (FFNN), similar to the wide and deep models in Cheng et al. (2016). One tower is a standard deep FFNN, containing an embedding module, fully connected layers and a softmax classification layer. This tower is regularized with L2 loss. The other is a shallow layer that directly connects the one-hot token encodings to the softmax classification layer with a linear layer. This tower is regularized with a sparse L1 loss. The shallow tower provides a direct method to learn task-specific priors over the classes for the tokens.

We allow the controller to select among pre-trained embedding modules for the input to the model. This has two benefits: first, the quality of the child models on smaller datasets improves, and second, it decreases convergence time of the child models. The latter is critical because training many child models in AML has high computational cost.

The single search space for all tasks is defined by the following sequence of choices: 1) The pre-trained input embed-

ding module. 2) Whether to fine tune the input embedding module. 3) The number of hidden layers. 4) The hidden layers size. 5) The hidden layers activation function. 6) Which layer normalization scheme to use (if any). 7) Dropout rate for the hidden layers. 8) The learning rate for the deep network. 9) Regularization strength for the deep layers. 10) The learning rate for the shallow network. 11) Regularization strength for the shallow layer. 12) The number of training steps. The Appendix contains the exact specification. All models are trained using the Proximal Adagrad optimizer with batches size 100. Despite restricting to simple child models the search space contains 1.1B configurations.

**Controller model** The controller consists of a 2-layer LSTM with 50 units. The action and task embeddings have size 25. The controller and embedding weights are initialized uniformly at random, yielding an approximately uniform distribution over actions. The controller’s learning rate is set to  $10^{-4}$  and it receives gradient updates after every child completes (batch size 1).

Previous works in neural search with reinforcement learning used the REINFORCE algorithm (Zoph & Le, 2017), and more recently, PPO (Zoph et al., 2017; Bello et al., 2017). We tried four variants of policy gradient to train the controller: vanilla REINFORCE (Williams, 1992), TRPO (Schulman et al., 2015), UREX (Nachum et al., 2017) and PPO (Schulman et al., 2017). On a pilot study on four NLP tasks we found REINFORCE and TRPO to performed best and selected REINFORCE for the following experiments.

### 4.2. Natural Language Processing

**Data** We evaluate using 21 text classification tasks. These differ in the number of examples, text length and class count. Table 1 contains an summary of the data, details and links to their sources are presented in the Appendix. The child models are trained on the training set. Their accuracy on the validation set is used as reward for the controller. After model search is finished, the child models with the best validation accuracies are evaluated on the test set. For the datasets that do not define a train/validation/test split, we split randomly 80/10/10.

**Metrics** To evaluate the ability of AML to find good configurations we compute the accuracy of the best child models generated during the search. To reduce noise introduced during training and evaluation of the child models we average the performance of the best N models found. These best N models are selected according to accuracy on validation set. We refer to the validation/test accuracy of these N models as validation/test ‘accuracy-topN’, respectively. To assess convergence rates we use two metrics: accuracy-topN given a fixed budget of trials and the number of trials required to attain a certain level of performance. The latter can only



Table 1. Statistics for the NLP classification datasets: number of examples, number of classes, length of the text in characters. Further details are in the Appendix.

Dataset	Examples	Classes	Len (chars)
20 Newsgroups	18,864	20	2,000
Airline	14640	3	104
Brown Corpus	500	15	20,000
Complaints	183,334	157	1,000
Corp Messaging	3,118	4	121
Customer Reviews	3800	2	100
Economic News	7,991	2	1,400
Emotion	40,000	13	73
Disasters	10,860	2	101
Global Warming	4,225	2	112
Movie Subj	10,000	2	127
MPQA Opinion	10,606	2	19
News Aggregator	422,937	4	57
Sentiment Cine	3,878	2	2,760
Sentiment IMDB	50,000	2	1,360
Political Message	5,000	9	205
Primary Emotions	2,524	18	87
Prog Opinion	1,159	3	102
Sentiment SST	70,042	2	105
SMS Spam	5,573	2	81
US Economy	6,654	2	305

be used with validation accuracy-topN since test accuracy-topN does not necessarily increase monotonically with the number of trials.

### 4.3. Transfer Learning

We randomly sampled 8 of the 21 tasks (Complaints, News Aggregator, Airline, Economic News, Political Message, Primary Emotion, US Economy, Sentiment SST) to pre-train a multitask model. We then transfer from this model to each of the remaining 13 tasks and compare our proposed method, Transfer AML (T-AML), to random search (RS) and AML from scratch.

To assess directly the algorithms’ ability to optimize the reward (validation set accuracy) we compute the speed-up versus RS. We first compute accuracy-top10 on the validation set for RS given a fixed budget of  $T$  trials. We set  $T$  to 5000 for all datasets except for the Brown Corpus and 20 Newsgroups where we can only use a budget of 500 and 3500 trials, respectively, since these datasets were slower to train. We then report the number of trials required by AML and T-AML to achieve the same validation accuracy-top10 as RS with  $T$  trials. Table 2 shows the results. Note, RS will show fewer than 5000 trials if it converged before then. Ta-

Table 2. Number of trials needed to attain a validation accuracy-top10 equal to that random search with a fixed budget of  $T$  trials.  $T = 5000$  trials for all datasets except Brown and 20 Newsgroups for which we use 500/3500 respectively. Bolding indicates the best performing algorithm. n/a indicates that the algorithm did not achieve the desired accuracy in the allotted time.

Dataset	RS	AML	T-AML
20 Newsgroups	2845	n/a	<b>550</b>
Brown Corpus	465	n/a	<b>10</b>
SMS Spam	4815	3390	<b>70</b>
Corp Messaging	3850	1510	<b>80</b>
Disasters	4970	2730	<b>25</b>
Emotion	4995	1645	<b>195</b>
Global Warming	4985	1935	<b>90</b>
Prog Opinion	4200	3620	<b>60</b>
Customer Reviews	4895	925	<b>15</b>
MPQA Opinion	4965	1510	<b>15</b>
Sentiment Cine	4520	3225	<b>535</b>
Sentiment IMDB	4760	<b>630</b>	690
Movie Subj	4745	1600	<b>105</b>

ble 2 shows that T-AML is highly effective in optimizing the validation accuracy. In all but one cases T-AML achieves the desired reward over an order of magnitude faster than AML.

Next, we assess the quality of the discovered models on the test set. Table 3 shows test accuracy-top10 after a fixed budget of 2000 trials (500 for Brown Corpus). The table shows that within this budget T-AML performs best, or joint best on all but one dataset. T-AML outperforms single task AML on 10 out of the 13 datasets, ties on 1, and loses on 2. On the datasets where T-AML does not produce the best final model at 2000 trials, it often produces better model at earlier iterations. Figure 2 shows the full learning curves of test set accuracy-top10 versus number of trials. The Appendix contains the validation accuracy-top10 curves. Figure 2 shows that in most cases the controller with transfer starts with a much better prior over good models. On some datasets the quality is improved with further training e.g. Emotion, Corp Messaging, but in others the initial configurations learned from the multitask model are not improved upon.

### 4.4. Multitask Training

We now present more details on the multitask pre-training of the controller. Table 4 shows the test set accuracy-top10 of RS, single task AML and Multitask AML (M-AML) given a budget of 2000 trials per task.

Single task AML outperforms random search on only 5 of the 8 datasets. Multitask-AML yields a moderate perform

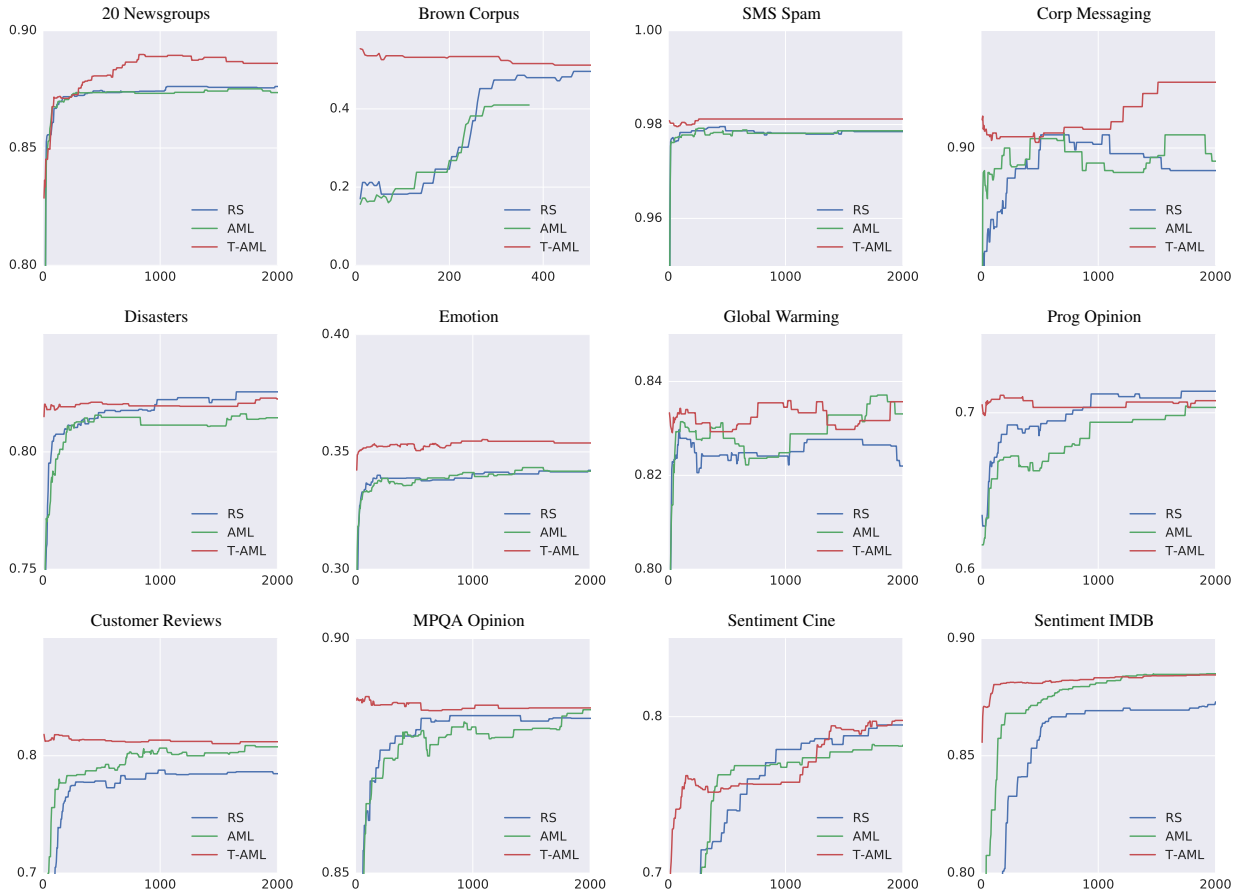


Figure 2. Learning curves for transfer learning. Average test set accuracy of the 10 models with best validation accuracy (test accuracy-top10) found up to each trial.

increase over single task training, performing best or joint best on 6 datasets and outperforms RS on 7 datasets.

Our primary objective is not to achieve state of the art on all datasets, but to get good performance automatically with fewest possible trials. Our search space, although large, does not contain many high-performing components (for example convolutions). Also, our use of embedding modules pre-trained on large datasets may give our methods an advantage over previous results. However, to check that we are generating good models with AML we check some previous published results where available. Almeida et al. (2013) use classical ML classifiers (Logistic Regression, SVMs, etc.) on SMS Spam and report best accuracy of 97.59%. T-AML gets accuracy-top10 of 98.1%. Le & Mikolov (2014) report 92.58% accuracy on Sentiment IMDB which is greater than T-AML, but they include more complex architectures not in the AML search space. Li et al. (2016) report 86.8% accuracy using an ensemble of weighted neural BOWs on MPQA. M-AML and T-AML achieve accuracy-top10 of

88.5%. Li et al. (2016) also evaluate their ensemble of weighted neural BOW models on customer reviews, and achieve 82.5% best accuracy, though the best accuracy of any single model is 81.1%. Comparably, M-AML gets an accuracy-top10 of 80.8% and T-AML gets an accuracy-top10 of 81.2%. Barnes et al. (2017) compare many algorithms and report best accuracy on Sentiment-SST of 83.1% using LSTMs. M-AML gets an accuracy-Top10 of 83.4%. The best performance achieved with a more complex architecture that is not within the scope of the described AML search space is: 87.8% (Le & Mikolov, 2014). Maas et al. (2011) report 88.1% on Movie Subj, T-AML gets accuracy-top10 of 93.3%.

#### 4.5. Image classification

To validate the generality of our approach we apply it to image classification. We train 2 AML controllers on the Cifar-10 task. The first is trained from scratch, and the second pre-trained on 2 other image classification tasks:

Table 3. Accuracy-top10 on the test set given at a fixed budget. Error bars show  $\pm 2$  s.e.m. computed across the top 10 models. S.e.m. only shown on T-AML due to space constraints, similar values were observed on the other datasets. Bolding indicates the best performing algorithm and those within 2 s.e.m. of the best.

Dataset	RS	AML	T-AML
20 Newsgroups	87.6	87.4	<b>88.6 <math>\pm 0.5</math></b>
Brown Corpus	49.6	41.0	<b>51.2 <math>\pm 2.8</math></b>
SMS Spam	97.8	97.9	<b>98.1 <math>\pm 0.1</math></b>
Corp Messaging	89.6	89.8	<b>91.1 <math>\pm 0.6</math></b>
Disasters	<b>82.6</b>	81.5	<b>82.3 <math>\pm 0.4</math></b>
Emotion	34.2	34.2	<b>35.4 <math>\pm 0.2</math></b>
Global Warming	82.2	<b>83.3</b>	<b>83.6 <math>\pm 0.7</math></b>
Prog Opinion	<b>71.4</b>	70.3	<b>70.8 <math>\pm 0.6</math></b>
Customer Reviews	78.5	<b>80.8</b>	<b>81.2 <math>\pm 0.5</math></b>
MPQA Opinion	<b>88.3</b>	<b>88.5</b>	<b>88.5 <math>\pm 0.3</math></b>
Sentiment Cine	<b>79.5</b>	78.1	<b>79.8 <math>\pm 1.1</math></b>
Sentiment IMDB	87.3	<b>88.5</b>	<b>88.4 <math>\pm 0.1</math></b>
Movie Subj	93.1	<b>93.6</b>	93.3 $\pm 0.2$

MNIST and Flowers<sup>1</sup>. Datasets details contained in the Appendix. Figure 3 shows the mean accuracy on the test set of the top 10 models according to the validation accuracy. The test accuracy of the single best model chosen on the validation set is: 95.26% for AML and 97.13% for T-AML. To the best of our knowledge, the state of the art Cifar-10 model trained from scratch is 96.6% (Huang et al., 2017). Our result is not directly comparable because T-AML may use embedding modules (layers) pre-trained on larger datasets. However, it verifies that T-AML is able to find highly performant models automatically. We observe that the controller learns to prefer to embed the image with a Inception v3 network pre-trained on ImageNet and activated for fine tuning. It prefers the Swish activation (Ramachandran et al., 2017) over Relu and selects a dropout rate of 0.3.

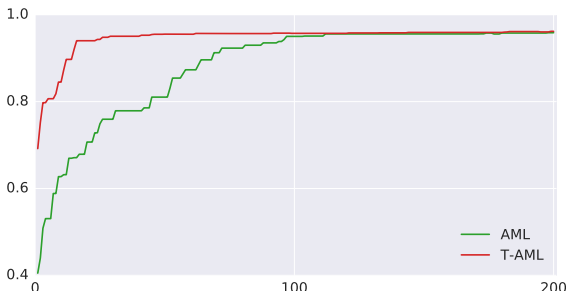


Figure 3. Comparison on Image classification task, Cifar 10. Mean test accuracy of the top 10 models chosen on the validation set.

<sup>1</sup>goo.gl/tpzfR1

Table 4. Accuracy-top10 on the test set given at a fixed budget of 2000 trials (500 for Brown Corpus). The number of trials per task is equal for all algorithms. Error bars show  $\pm 2$  s.e.m. computed across the top 10 models.

Dataset	RS	AML	M-AML
Complaints	49.9	49.7	<b>52.5 <math>\pm 0.3</math></b>
News Aggregator	93.0	<b>93.8</b>	<b>93.8 <math>\pm 0.1</math></b>
Airline	81.7	82.3	<b>82.8 <math>\pm 0.2</math></b>
Economic News	<b>81.1</b>	<b>81.2</b>	80.6 $\pm 0.4$
Political Message	<b>43.2</b>	<b>42.6</b>	<b>43.2 <math>\pm 0.6</math></b>
Primary Emotion	26.3	27.2	<b>28.1 <math>\pm 0.9</math></b>
US Economy	73.9	73.7	<b>75.0 <math>\pm 0.3</math></b>
Sentiment SST	82.7	<b>83.6</b>	<b>83.4 <math>\pm 0.7</math></b>

#### 4.6. Further Analysis

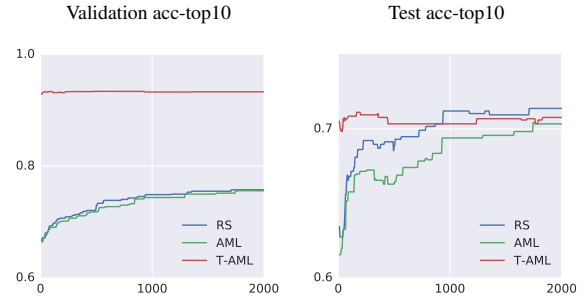


Figure 4. Left: validation, Right: test accuracy-top10 on Progressive Opinion dataset.

**Potential to overfit during meta-learning** Overfitting is a central focus in ML. However, the overfitting of a meta-learner performing AML is not yet widely addressed. This is likely because AML is computationally expensive and many trials are required to overfit the validation set. However, in our experiments we observe that this occurs in some cases. This can be observed in Figure 4 which shows the accuracy-top10 on the validation and test sets for the Progressive Opinion dataset. Although the T-AML attains better solutions in the first few trials, its test performance does not improve further, and the generalization gap between the validation and test accuracy-top10 is large. This is the most extreme case we observed, the other datasets exhibit a smaller validation/test gap (see the Appendix for all of the validation curves). This effect is pronounced on Progressive Opinion because its validation set is very small, with only 116 examples.

Other than applying entropy regularization to the controller’s policy, we leave investigation into combating overfitting in meta-learning for future research. Here, we simply

emphasize that as AML methods extend to large numbers of datasets as in this work, some of which may be small, that meta-overfitting becomes a pertinent topic.

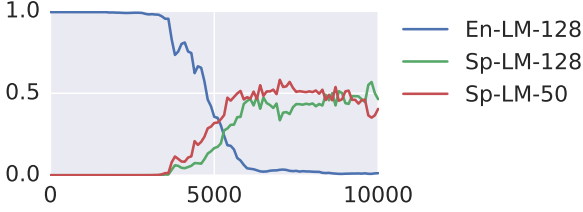


Figure 5. Evolution of the choice of pre-trained embeddings when transferring to the Spanish Corpus-Cine task. y-axis indicates the probability of sampling each table as a function of trial number. Only the most probably three tables are plotted.

**Transfer across languages** The Sentiment Cine task is an outlier because it contains only Spanish text. All of the other tasks are in English, including those used in the pre-trained multitask controller. As expected, transfer from the English tasks to Sentiment Cine does not perform as well as for the other English tasks. Both the reward being optimized (validation accuracy) and the test set performance is relatively low compared to the baselines, Figure 2.

The most language-sensitive parameters are the pre-trained word embedding modules. We allow the controller to select from eight pretrained embeddings. These vary in dimensionality, training algorithm (skip-gram, CBOW, language modelling), training data (Wikipedia or news), and language (En or Es). Details in the appendix. Six of the tables are English, the other two Spanish. For all tasks, the multitask controller selects one of the English embeddings with high probability ( $> 0.99$ ). We observed that in the first 2000 iterations the when the controller is transferred to Sentiment Cine it also chooses the English embeddings. However, after training for longer we observe that the controller is able to switch after 5k iterations, Figure 5. This indicates that although transfer works better on more similar tasks, the controller is still able to adapt to outliers given sufficient training time.

**Task representations and learned distributions** We inspect the learned similarity between the tasks via their embeddings. Figure 6 shows the cosine similarity between the eight task embeddings learned during multitask training. It is hard to guess *a priori* which tasks would be similar; the number of examples, classes and text length differ greatly 1. However, Multitask-AML appears to learn clusters of tasks that have similar high performing configurations.

At convergence, the tasks in the cluster {Complaints, New Agg, Airline, Primary Emotion} are assigned 1-layer net-

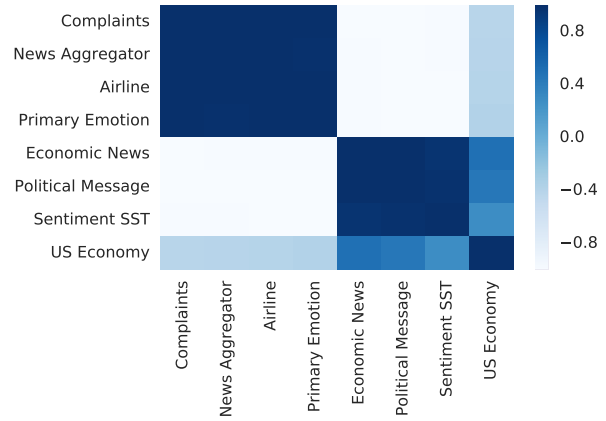


Figure 6. Cosine similarity between the task embeddings learned by the multitask AML model.

works with 256 units and dropout rate 0.2 with high probability under the policy. The cluster {Economic News, Political Emotion, Sentiment SST} are assigned 2-layer networks with 64 units and dropout 0.3

Some choices are common to all tasks. For example, the same 128-dimension word embeddings are chosen, and the controller always chooses to fine-tune them. The controller has the options to switch off either the to deep or shallow tower in the children by setting the regularization very high. However, in all cases it chooses to keep both active.

## 5. Conclusion

Machine learning practitioners design good models by leveraging prior knowledge obtained from prior tasks. Automated machine learning should also learn from the models they have discovered for prior tasks. We show that transfer AML yields substantially faster convergence than training from scratch. We also show that by pre-training multiple tasks simultaneously, sample efficiency is improved and AML learns task embeddings that encode meaningful relationships between tasks. AML enables practitioners to train effective models with minimal human tuning; the practitioner need only define a single search space for all tasks. However, it comes with high computational costs. This paper presents a promising approach to reducing this cost and making AML more generally useful.

## References

- Almeida, Tiago, Hidalgo, José María Gómez, and Silva, Tiago Pasqualini. Towards sms spam filtering: Results under a new dataset. *International Journal of Information Security Science*, 2013.



- Baker, Bowen, Gupta, Otkrist, Naik, Nikhil, and Raskar, Ramesh. Designing neural network architectures using reinforcement learning. *arXiv preprint arXiv:1611.02167*, 2016.
- Baker, Bowen, Gupta, Otkrist, Naik, Nikhil, and Raskar, Ramesh. Designing neural network architectures using reinforcement learning. In *ICLR*, 2017.
- Barnes, Jeremy, Klinger, Roman, and Schulte im Walde, Sabine. Assessing state-of-the-art sentiment models on state-of-the-art sentiment datasets. In *Proceedings of the 8th Workshop on Computational Approaches to Subjectivity, Sentiment and Social Media Analysis*. ACL, 2017.
- Bello, Irwan, Zoph, Barret, Vasudevan, Vijay, and Le, Quoc V. Neural optimizer search with reinforcement learning. In *ICML*, 2017.
- Bergstra, James and Bengio, Yoshua. Random search for hyper-parameter optimization. *JMLR*, 13(Feb), 2012.
- Bergstra, James, Yamins, Daniel, and Cox, David. Making a science of model search: Hyperparameter optimization in hundreds of dimensions for vision architectures. In *ICML*, 2013.
- Bergstra, James S, Bardenet, Rémi, Bengio, Yoshua, and Kégl, Balázs. Algorithms for hyper-parameter optimization. In *NIPS*, 2011.
- Cai, Han, Chen, Tianyao, Zhang, Weinan, Yu, Yong, and Wang, Jun. Reinforcement learning for architecture search by network transformation. *arXiv preprint arXiv:1707.04873*, 2017.
- Cheng, Heng-Tze, Koc, Levent, Harmsen, Jeremiah, Shaked, Tal, Chandra, Tushar, Aradhye, Hrishi, Anderson, Glen, Corrado, Greg, Chai, Wei, Ispir, Mustafa, Anil, Rohan, Haque, Zakaria, Hong, Lichan, Jain, Vihan, Liu, Xiaobing, and Shah, Hemal. Wide & deep learning for recommender systems. *CoRR*, abs/1606.07792, 2016.
- Conti, Edoardo, Madhavan, Vashisht, Such, Felipe Petroski, Lehman, Joel, Stanley, Kenneth O, and Clune, Jeff. Improving exploration in evolution strategies for deep reinforcement learning via a population of novelty-seeking agents. *arXiv preprint arXiv:1712.06560*, 2017.
- Feurer, Matthias, Springenberg, Jost Tobias, and Hutter, Frank. Initializing bayesian hyperparameter optimization via meta-learning. In *AAAI*, 2015.
- Finn, Chelsea, Abbeel, Pieter, and Levine, Sergey. Model-agnostic meta-learning for fast adaptation of deep networks. *arXiv preprint arXiv:1703.03400*, 2017.
- Greensmith, Evan, Bartlett, Peter L, and Baxter, Jonathan. Variance reduction techniques for gradient estimates in reinforcement learning. *JMLR*, 5(Nov), 2004.
- Huang, Gao, Liu, Zhuang, and Weinberger, Kilian Q. Densely connected convolutional networks. *CVPR*, 2017.
- Kirkpatrick, James, Pascanu, Razvan, Rabinowitz, Neil, Veness, Joel, Desjardins, Guillaume, Rusu, Andrei A, Milan, Kieran, Quan, John, Ramalho, Tiago, Grabska-Barwinska, Agnieszka, et al. Overcoming catastrophic forgetting in neural networks. *Proceedings of the National Academy of Sciences*, 2017.
- Le, Quoc and Mikolov, Tomas. Distributed representations of sentences and documents. In *ICML*, ICML'14, 2014.
- Li, Bofang, Zhao, Zhe, Liu, Tao, Wang, Puwei, and Du, Xiaoyong. Weighted neural bag-of-n-grams model: New baselines for text classification. In *Proceedings of COLING 2016, the 26th International Conference on Computational Linguistics: Technical Papers*, 2016.
- Maas, Andrew L., Daly, Raymond E., Pham, Peter T., Huang, Dan, Ng, Andrew Y., and Potts, Christopher. Learning word vectors for sentiment analysis. In *ACL: Human Language Technologies*. ACL, 2011.
- Miikkulainen, Risto, Liang, Jason Zhi, Meyerson, Elliot, Rawal, Aditya, Fink, Dan, Francon, Olivier, Raju, Bala, Shahrzad, Hormoz, Navruzian, Arshak, Duffy, Nigel, and Hodjat, Babak. Evolving deep neural networks. *CoRR*, abs/1703.00548, 2017.
- Mishra, Nikhil, Rohaninejad, Mostafa, Chen, Xi, and Abbeel, Pieter. A simple neural attentive meta-learner. In *NIPS 2017 Workshop on Meta-Learning*, 2017.
- Nachum, Ofir, Norouzi, Mohammad, and Schuurmans, Dale. Improving policy gradient by exploring under-appreciated rewards. In *ICLR*, 2017.
- Negrinho, Renato and Gordon, Geoff. Deeparchitect: Automatically designing and training deep architectures. *arXiv preprint arXiv:1704.08792*, 2017.
- Prajit Ramachandran, Barret Zoph, Quoc V. Le. Searching for activation functions, 2018.
- Ramachandran, Prajit, Zoph, Barret, and Le, Quoc V. Swish: a self-gated activation function. *arXiv preprint arXiv:1710.05941*, 2017.
- Real, Esteban, Moore, Sherry, Selle, Andrew, Saxena, Saurabh, Suematsu, Yutaka Leon, Le, Quoc, and Kurakin, Alex. Large-scale evolution of image classifiers. In *ICML*, 2017.

- Schulman, John, Levine, Sergey, Abbeel, Pieter, Jordan, Michael, and Moritz, Philipp. Trust region policy optimization. In *ICML*, 2015.
- Schulman, John, Wolski, Filip, Dhariwal, Prafulla, Radford, Alec, and Klimov, Oleg. Proximal policy optimization algorithms. *arXiv preprint arXiv:1707.06347*, 2017.
- Sharif Razavian, Ali, Azizpour, Hossein, Sullivan, Josephine, and Carlsson, Stefan. Cnn features off-the-shelf: an astounding baseline for recognition. In *CVPR workshops*, 2014.
- Snoek, Jasper, Larochelle, Hugo, and Adams, Ryan P. Practical bayesian optimization of machine learning algorithms. In *NIPS*, 2012.
- Such, Felipe Petroski, Madhavan, Vashisht, Conti, Edoardo, Lehman, Joel, Stanley, Kenneth O, and Clune, Jeff. Deep neuroevolution: Genetic algorithms are a competitive alternative for training deep neural networks for reinforcement learning. *arXiv preprint arXiv:1712.06567*, 2017.
- Teh, Yee Whye, Bapst, Victor, Czarnecki, Wojciech Marian, Quan, John, Kirkpatrick, James, Hadsell, Raia, Heess, Nicolas, and Pascanu, Razvan. Distal: Robust multitask reinforcement learning. *arXiv preprint arXiv:1707.04175*, 2017.
- Wichrowska, Olga, Maheswaranathan, Niru, Hoffman, Matthew W, Colmenarejo, Sergio Gomez, Denil, Misha, de Freitas, Nando, and Sohl-Dickstein, Jascha. Learned optimizers that scale and generalize. *arXiv preprint arXiv:1703.04813*, 2017.
- Williams, Ronald J. Simple statistical gradient-following algorithms for connectionist reinforcement learning. In *Reinforcement Learning*. Springer, 1992.
- Yosinski, Jason, Clune, Jeff, Bengio, Yoshua, and Lipson, Hod. How transferable are features in deep neural networks? In *NIPS*, 2014.
- Zhan, Yusen and Taylor, Matthew E. Online transfer learning in reinforcement learning domains. *arXiv preprint arXiv:1507.00436*, 2015.
- Zhong, Zhao, Yan, Junjie, and Liu, Cheng-Lin. Practical network blocks design with q-learning. In *AAAI*, 2018.
- Zoph, Barret and Le, Quoc V. Neural architecture search with reinforcement learning. In *ICLR*, 2017.
- Zoph, Barret, Vasudevan, Vijay, Shlens, Jonathon, and Le, Quoc V. Learning transferable architectures for scalable image recognition. *CoRR*, abs/1707.07012, 2017.

# Supplementary Material for Transfer Automatic Machine Learning

March 2, 2018

This document contains a description of the search space used in our experiments (Table 1), details of the pretrained modules for embedding text and images (Tables 2 and 3), and statistics for the datasets used (Table 4 and 5). It also contains the learning curves for Transfer AML (Figures 1 and 2) and Multitask AML (Figures 3 and 4) on the validation and test sets.

Table 1: The search space for our AML models.

Parameter	Search Space
1) Input embedding modules	Text input: refer to Table 2. Image input: refer to Table 3.
2) Fine-tune input embedding module	{True, False}
3) Number of hidden layers	{1, 2, 3, 5, 7}
4) Hidden layers size	{8, 16, 32, 64, 128, 256}
5) Hidden layers activation	{relu, swish}
6) Hidden layers normalization	{none, batch norm, layer norm}
7) Hidden layers dropout rate	{0.0, 0.01, 0.05, 0.1, 0.2, 0.3, 0.4, 0.5, 0.6}
8) Deep tower learning rate	{0.001, 0.003, 0.01, 0.03, 0.1, 0.3, 1.0, 3.0}
9) Deep tower regularization weight	{0.0, 0.00001, 0.0001, 0.001, 0.01, 0.1, disable deep tower}
10) Wide tower learning rate	{0.001, 0.003, 0.01, 0.03, 0.1, 0.3, 1.0, 3.0}
11) Wide tower regularization weight	{0.0, 0.00001, 0.0001, 0.001, 0.01, 0.1, disable wide tower}
12) Number of training samples	{1000, 3000, 10000, 30000, 100000, 300000, 1000000}

Table 2: Options for text input embedding modules. These are pre-trained text embedding tables, trained on datasets with different languages and size. The text input to these modules is tokenized according to the module dictionary and normalized by lower-casing and stripping rare characters. The embeddings of each token are aggregated with a mean BOW approach.

Language/ID	Dataset size (tokens)	Embedding dimensions	Vocab. size	Training algorithm
Spanish-small	50B	50	995k	Language model
Spanish-big	50B	128	995k	Language model
English-small	7B	50	982k	Language model
English-big	200B	128	999k	Language model
English-wiki-small	4B	250	1M	Skipgram
English-wiki-big	4B	500	1M	Skipgram
English-news-small	90B	100	5.9M	CBOW, negative sampling
English-news-big	90B	500	5.9M	CBOW, negative sampling

Table 3: Options for image input embedding modules. To map an image, the controller can choose among state of the art architectures pre-trained on ImageNet. The module consists in the pre-trained model up to the final layer of logits.

Architecture	Dataset	Reference
MobileNet v1	Imagenet	(Howard et al., 2017)
Inception v2	Imagenet	(Ioffe & Szegedy, 2015)
Inception v3	Imagenet	(Szegedy et al., 2015)
Resnet v1.101	Imagenet	(He et al., 2015)
Resnet v1.50	Imagenet	(He et al., 2015)

Table 4: Statistics and references for the NLP classification tasks.

Dataset	Train samples	Valid. samples	Test samples	Classes	Lang (chars)	Len	Reference
20 Newsgroups	15,076	1,885	1,885	20	En	2,000	(Lang, 1995)
Airline	11,712	1,464	1,464	3	En	104	crowdflower.com
Brown Corpus	400	50	50	15	En	20,000	(Francis & Kuera, 1982)
Complaints	146,667	18,333	18,334	157	En	1,000	catalog.data.gov
Corp Messaging	2,494	312	312	4	En	121	crowdflower.com
Customer Reviews	3,044	378	378	2	En	100	(Hu & Liu, 2004)
Disasters	8,688	1,086	1,086	2	En	101	crowdflower.com
Economic News	6,392	799	800	2	En	1,400	crowdflower.com
Emotion	32,000	4,000	4,000	13	En	73	crowdflower.com
Global Warming	3,380	422	423	2	En	112	crowdflower.com
Movie Subj	8052	972	976	2	En	127	(Pang et al., 2002)
MPQA Opinion	8,547	1,025	1,034	2	En	19	(Deng & Wiebe, 2015)
News Aggregator	338,349	42,294	42,294	4	En	57	(Lichman, 2013)
Political Message	4,000	500	500	9	En	205	crowdflower.com
Primary Emotions	2,019	252	253	18	En	87	crowdflower.com
Prog Opinion	927	116	116	3	En	102	crowdflower.com
Sentiment Cine	3119	382	377	2	Spanish	2,760	(Cruz et al., 2008)
Sentiment IMDB	19946	5054	25000	2	En	1,360	(Maas et al., 2011)
Sentiment SST	67,349	872	1,821	2	En	105	(Socher et al., 2013)
SMS Spam	4,459	557	557	2	En	81	(Almeida et al., 2011)
US Economy	3,961	495	495	2	En	305	crowdflower.com

Table 5: Statistics and references for the Image classification tasks.

Dataset	Train samples	Valid. samples	Test samples	Classes	Image size	Reference
Cifar 10	45000	5000	10000	10	32x32x3	(Krizhevsky et al.)
Mnist	55000	5000	10000	10	28x28x1	(LeCun & Cortes, 2010)
Flowers	2018	552	550	5	variablex3	goo.gl/tpzfr1



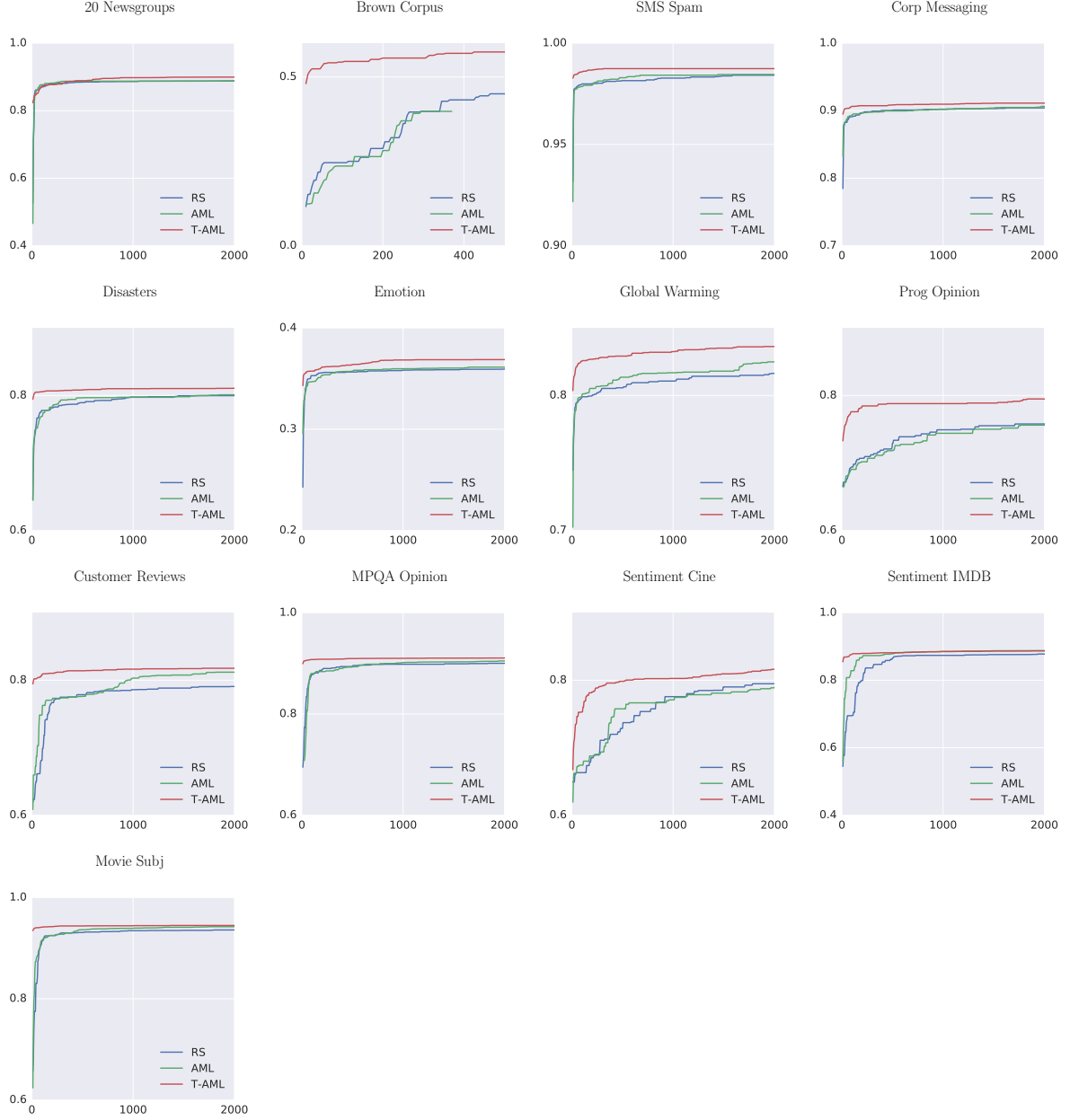


Figure 1: Learning curves for transfer learning. X-axis depicts number of trials (T) performed for each task. Y-axis depicts the mean validation accuracy of the 10 models achieving top validation accuracy (validation accuracy-top10).

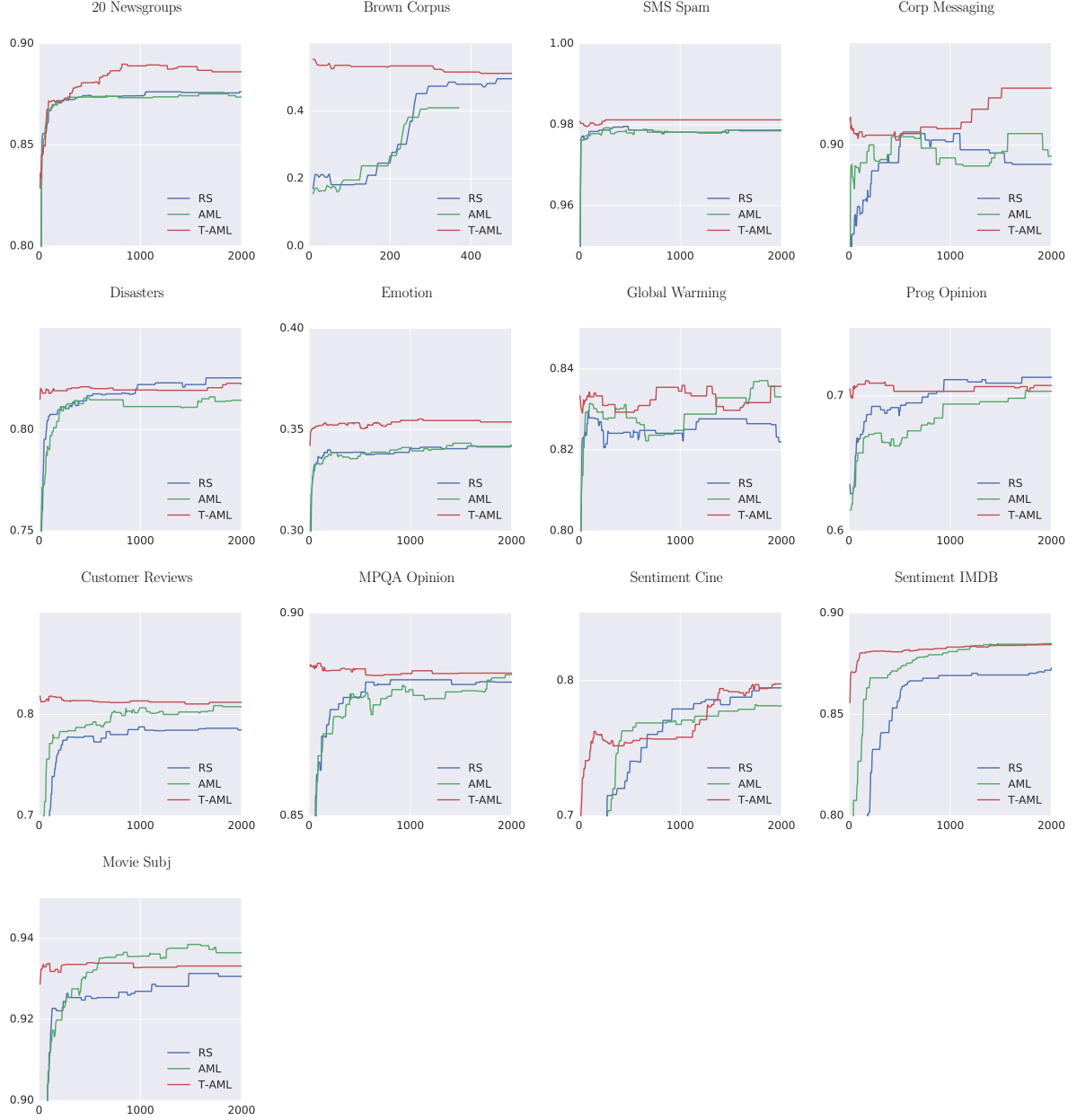


Figure 2: Learning curves for transfer learning. X-axis depicts number of trials (T) performed for each task. Y-axis depicts the mean test accuracy of the 10 models achieving top validation accuracy (test accuracy-top10).

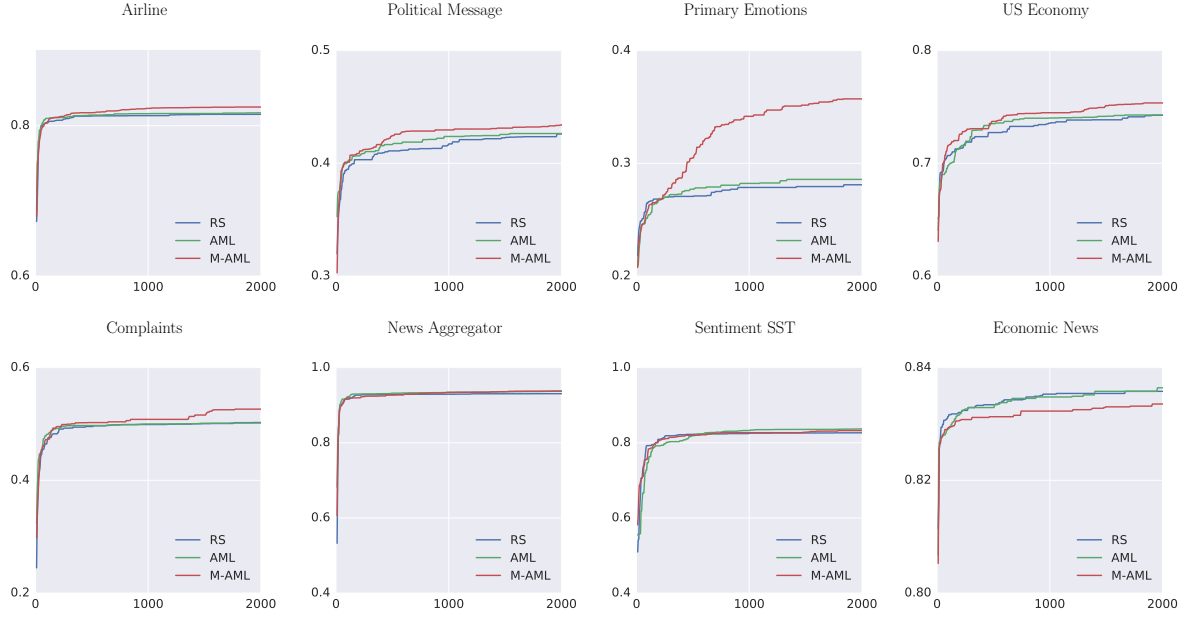


Figure 3: Learning curves for multitask training. X-axis depicts number of trials (T) performed for each task. Y-axis depicts the mean validation accuracy of the 10 models achieving top validation accuracy (validation accuracy-top10).

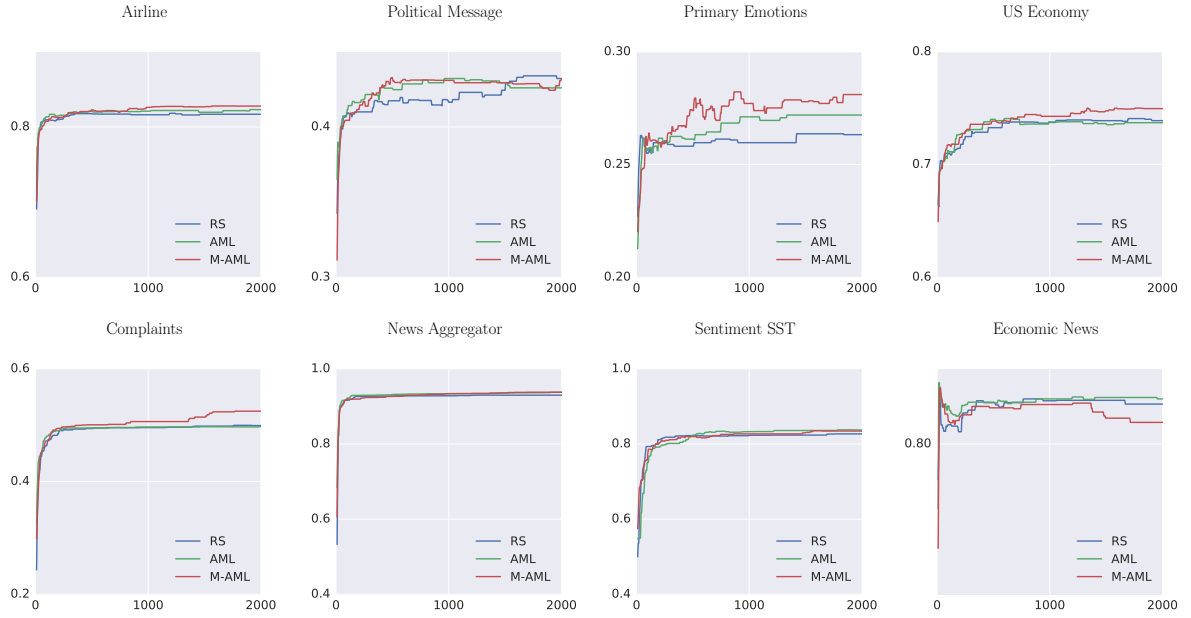


Figure 4: Learning curves for multitask training. X-axis depicts number of trials (T) performed for each task. Y-axis depicts the mean test accuracy of the 10 models achieving top validation accuracy (test accuracy-top10).

## References

- Almeida, Tiago A., Hidalgo, José María G., and Yamakami, Akebo. Contributions to the study of sms spam filtering: New collection and results. In *Proceedings of the 11th ACM Symposium on Document Engineering, DocEng '11*, New York, NY, USA, 2011. ACM.
- Cruz, Fermín L, Troyano, Jose A, Enriquez, Fernando, and Ortega, Javier. Clasificación de documentos basada en la opinión: experimentos con un corpus de criticas de cine en espanol. *Procesamiento del lenguaje natural*, 2008.
- Deng, Lingjia and Wiebe, Janyce. Mpqa 3.0: Entity/event-level sentiment corpus. In *ACL*, Denver, Colorado, USA, 2015. Sociedad Española para el Procesamiento del Lenguaje Natural.
- Francis, W. Nelson and Kuera, Henry. Frequency analysis of english usage. lexicon and grammar. In *Houghton Mifflin*, 1982.
- He, Kaiming, Zhang, Xiangyu, Ren, Shaoqing, and Sun, Jian. Deep residual learning for image recognition. *CoRR*, abs/1512.03385, 2015.
- Howard, Andrew G., Zhu, Menglong, Chen, Bo, Kalenichenko, Dmitry, Wang, Weijun, Weyand, Tobias, Andreetto, Marco, and Adam, Hartwig. Mobilenets: Efficient convolutional neural networks for mobile vision applications. *CoRR*, abs/1704.04861, 2017. URL <http://arxiv.org/abs/1704.04861>.
- Hu, Mingqing and Liu, Bing. Mining and summarizing customer reviews. In *Proceedings of the Tenth ACM SIGKDD International Conference on Knowledge Discovery and Data Mining, KDD '04*, New York, NY, USA, 2004. ACM.
- Ioffe, Sergey and Szegedy, Christian. Batch normalization: Accelerating deep network training by reducing internal covariate shift. *CoRR*, abs/1502.03167, 2015.
- Krizhevsky, Alex, Nair, Vinod, and Hinton, Geoffrey. Cifar-10 (canadian institute for advanced research).
- Lang, Ken. Newsweeder: Learning to filter netnews. In *ICML*, 1995.
- LeCun, Yann and Cortes, Corinna. MNIST handwritten digit database. 2010.
- Lichman, M. UCI machine learning repository, 2013.
- Maas, Andrew L., Daly, Raymond E., Pham, Peter T., Huang, Dan, Ng, Andrew Y., and Potts, Christopher. Learning word vectors for sentiment analysis. In *ACL: Human Language Technologies*. ACL, 2011.
- Pang, Bo, Lee, Lillian, and Vaithyanathan, Shivakumar. Thumbs up?: Sentiment classification using machine learning techniques. In *EMNLP*, Stroudsburg, PA, USA, 2002. ACL.
- Socher, Richard, Perelygin, Alex, Wu, Jean, Chuang, Jason, Manning, Christopher D., Ng, Andrew, and Potts, Christopher. Recursive deep models for semantic compositionality over a sentiment treebank. In *EMNLP*. ACL, 2013.
- Szegedy, Christian, Vanhoucke, Vincent, Ioffe, Sergey, Shlens, Jonathon, and Wojna, Zbigniew. Rethinking the inception architecture for computer vision. *CoRR*, abs/1512.00567, 2015.